Biointerface Research in Applied Chemistry
Platinum Open Access Journal (ISSN: 2069-5837)

Article
Volume 11, Issue 4, 2021, 11404 - 11417
https://doi.org/10.33263/BRIAC114.1140411417

Quantitative Estimation of D-Penicillamine in Pure and Pharmaceutical Samples Using Inhibitory Kinetic Spectrophotometric Method

Abhishek Srivastava [1,*]

[1] Department of Chemistry, GLA University, Mathura, U.P., India
* Correspondence: aabhichem@gla.ac.in;

Scopus Author ID 57191574287

Received: 19.11.2020; Revised: 6.12.2020; Accepted: 8.12.2020; Published: 11.12.2020

Abstract: Sulfur is the key element in a large number of drugs and bioactive molecules. Organo-sulfur compounds inhibit the catalytic efficiency of Hg^{2+} by forming a stable complex with it. The Hg^{2+} catalyzed exchange rate of cyanide with pyrazine from $[Ru(CN)_6]^{4-}$ will be reduced by the addition of the sulfur-containing drug, D-penicillamine (D-PCN). This inhibitory property of D-PCN can be employed for its micro-level kinetic determination. Optimum reaction condition viz. Temperature = 45.0 ± 0.1 °C, I = 0.1 M (KCl), $[Hg^{+2}] = 1.5 \times 10^{-4}$ M, [pyrazine] = 7.5×10^{-4} M, pH = 4.0 ± 0.02, and $[Ru(CN)_6^{4-}] = 5.25 \times 10^{-5}$ M were utilized to investigate the kinetic measurements at 370 nm (λ_{max} of $[Ru(CN)_5\ Pz]^{3-}$ complex). To acknowledge the inhibition induced by D-PCN on Hg^{2+} catalyzed substitution of cyanide with pyrazine from $[Ru(CN)_6]^{4-}$, a modified mechanistic scheme has been proposed. D-PCN can be quantitatively determined up to 1.0×10^{-6} M level by the proposed analytical method. The methodology can be economically and effectively employed for the quantitative determination of D-PCN in different samples. This methodology can also be convincingly adopted for the quick determination of D-PCN in the pharmaceutical samples with good accuracy and reproducibility. The addition of common excipients in pharmaceuticals even up to 1000 times with [D-PCN] does not interfere significantly in the estimation of D-PCN.

Keywords: ligand substitution reaction; inhibitory effect; D-penicillamine; hexacyanoruthenate(II); catalyst inhibitor complex; pharmaceutical preparations; excipients.

1. Introduction

Sulfur is an important element in a large number of drugs and bioactive molecules. Sulfur, present in a cell's enzymes and structural proteins, plays a key role in various metabolic processes [1-4]. Thus, developing an effective methodology to determine sulfur-containing drugs and bioactive molecules in distinct samples quantitatively is of huge importance and the pharmaceutical industry's demand. Penicillamine, a tri-functional organic moiety, contains carboxylic, amino, and thiol groups. Between the two enantiomeric forms, L- penicillamine is quite toxic [5], while D- penicillamine (D-PCN) has been listed as an essential medicine by World Health Organization and commercially sold with the trade names of Depen, Aaramine, Pendramine, Artin, Cuprenyl, and Cuprimine. D-PCN is a strong chelating agent and is effectively used to treat Wilson's disease by forming a stable complex with iron and copper and subsequently removing them via the kidney, in urine [6]. Chang *et al*. reported that the high dose zinc sulfate combined with low dose D-penicillamine is effective and safe for treating

pediatric Wilson disease [7]. D-penicillamine has been extensively used to treat mild/moderate lead poisoning via oral chelation therapy [8-9]. Results showed that the lower D-PCN dose reduces its adverse effects without significantly affecting the drug's efficacy [10]. Penicillamine protected Ag_{20} nanoclusters [11], penicillamine coated gold nanoparticles [12], penicillamine functionalized graphene [13]. Various D-penicillamine derivatives show great potential for the effective detection of Cu(II) ions in distinct samples, including human blood [14]. Zhang *et al*. developed a sensor containing D-penicillamine capped copper nanoparticles for histamine micro-level determination in red wine, pork, and fish [15]. It also reduces cystine excretion in cystinuria and can be used as a disease-modifying antirheumatic drug (DMARD) to treat the patient with severe active rheumatoid arthritis [16].

The kinetic investigation and mechanistic elucidation of catalyzed and uncatalyzed ligand exchange/oxidation reaction of transition metal complexes in an aqueous medium are fundamental [17-20]. The immediate applications of such reactions in synthetic and analytical chemistry attracted many environmentalists and chemists over the last century [21-22]. In this connection, numerous kinetic studies of coordinated cyanide from low-spin hexacyanoruthenate(II) with various ligands containing –N, -S, -P, and –O donor atoms were investigated by several authors [23-24].

Numerous literature is available to quantitatively estimate the sulfur-containing compounds in analytical and biological samples and pharmaceutical preparations [25-28]. The estimation methods include spectrophotometry [29,30], NMR-spectrometry [31], potentiometry [32], voltammetry [33], fluorimetry [34], flow injection analysis [35], chromatography [36-38], and colorimetry [25]. High cost for sample analysis, heavy instrumentation, time-consuming process, and high initial capital investment are the major disadvantages of most reported methods. A small number of kinetic records are present using different determination processes [39-41].

Ruthenium complexes with various bioactive molecules shows wide-range applications as DNA binder [42], Antitumor [43], Antileukemic [44], Immunosuppressant [45], Antimetastatic [46], Anticancer [47], Antiamebic [48], and Antifungal [49]. Several reports are available on the metal-catalyzed exchange of cyanide with nitrogen donor heterocyclic ligand from $[Ru(CN)_6]^{4-}$ in aqueous / surfactant medium [23,24]. The catalytic property of mercury (II) on the exchange of cyanide ligand with pyrazine from $[Fe(CN)_6]^{4-}$ has been successfully employed for the micro-level estimation of Hg(II) [50]. The stability of various metal complexes can be explained by the HSAB (hard-soft acid-base) concept. Organo-sulfur compounds inhibit the catalytic efficiency of Hg^{2+} by forming a stable complex with it [39-41]. This inhibitory function of organo-sulfur compounds can be employed for its kinetic determination at the micro-level. D-PCN suppresses the Hg^{2+} catalyzed substitution rate of cyanide with pyrazine from hexacyanoruthenate(II). This inhibitory property of D-PCN developed our interest to establish a precise and simple kinetic spectrophotometric method for the micro-level estimation of D-PCN. The current reaction system in hand produces more accurate results for the D-PCN determination. The uncatalyzed reaction between pyrazine and hexacyanoruthenate(II) is insignificant under the stipulated experimental condition [51]. The current communication deals with developing a new and accurate analytical method, which permits D-PCN estimation in various samples down to 1.0×10^{-6} M with good accuracy and reproducibility. This technique can also be convincingly utilized for the quick determination of D-PCN in pharmaceutical preparations.

2. Materials and Methods

2.1. Reagent used.

In all kinetic measurements, double deionized water and analytical-grade reagents were used. The weighed amount of $K_4[Ru(CN)_6].3H_2O$ (Sigma-Aldrich) and pyrazine (Merck) was used to prepare their stock solutions and kept in the dark to prevent their possible photo-degradation. D-penicillamine, procured from Hi-media, was used without further purification. Its dilution was done before the kinetic run to prevent the loss of Hg^{2+} via adsorption on the glass surface. KCl (CDH Fine Chemicals) was used to regulate the ionic strength (μ). At the same time, the pH of the reaction medium was managed by NaOH/HCl (Sigma-Aldrich). Potassium hydrogen phthalate procured from S D Fine Chemical Limited.

2.2. Instrumentation.

Mettler Toledo F20 digital pH meter was used to carry out pH measurements. The pH meter was calibrated with the predefined buffer solutions. All kinetic measurements were carried out on Lasany double beam microprocessor UV-Visible spectrophotometer model-LI-2700 by recording the hike in absorbance at 370 nm, the λ_{max} of stable yellow-colored $[Ru(CN)_5\ Pz]^{3-}$ complex.

2.3. Kinetic procedure.

No modification in absorbance was applied as only $[Ru(CN)_5\ Pz]^{3-}$ absorbs strongly. At the same time, the other reactants and catalysts show negligible absorption at this wavelength. All the reacting solutions were thermally equilibrated for 30 min at 45 °C and were mixed in the order of pyrazine, mercuric chloride, buffer, and KCl. Hexacyanoferrate(II) was injected lastly to initiate the substitution reaction. The absorbance values recorded with time at 370 nm were used to compute the initial reaction rate. The initial rate (the relative measure of reaction) was calculated by the slope of the graph plotted between absorbance and time. The influence of [pyrazine], ionic strength, $[Fe(CN)_6^{4-}]$, and temperature on substitution rate were discussed with the initial rate, whereas to address the influence of $[Hg^{2+}]$ and pH on reaction rate, the fixed time procedure was adopted.

2.4. Determination of D-Penicillamine.

The optimized reaction condition exhibiting an appreciable change in the absorbance values was judiciously selected from the detailed kinetic study [51]. All the reacting solutions viz., $[Hg^{+2}] = 1.5 \times 10^{-4}$ M, I=0.1 M (KCl), [pyrazine] = 7.5×10^{-4} M, buffer = 4.0 ± 0.02, $[Ru(CN)_6^{4-}] = 5.25 \times 10^{-5}$ M and D-PCN were thermally equilibrated for 30 min at 45 °C and were mixed rapidly in the sequence: pyrazine, mercuric chloride buffer solution, KCl, and D-PCN. Hexacyanoruthenate(II) solution was injected lastly to initiate the substitution reaction. The reaction mixture was vigorously shaken and transferred promptly to the spectrophotometric cuvette having a temperature-controlled cell compartment. The advancement of the indicator reaction was pursued by observing the hike in absorbance corresponding to the stable yellow-colored $[Ru(CN)_5Pz]^{3-}$ complex at 370 nm. A calibration plot drawn between the absorbance measured at 370 nm and varying [D-PCN] was used for the quantitative determination of D-PCN.

3. Results and Discussion

The Hg(II) promoted an exchange of CN^- with pyrazine from $[Ru(CN)_6]^{4-}$ results in a stable yellow-colored $[Ru(CN)_5\ Pz]^{3-}$ complex. The final product's slope ratio and mole ratio studies confirm that pyrazine and $[Ru(CN)_6]^{4-}$ reacts in a 1:1 mole ratio. Metal to ligand charge transfer (MLCT) complex is responsible for the strong absorption band for the product at 370 nm.

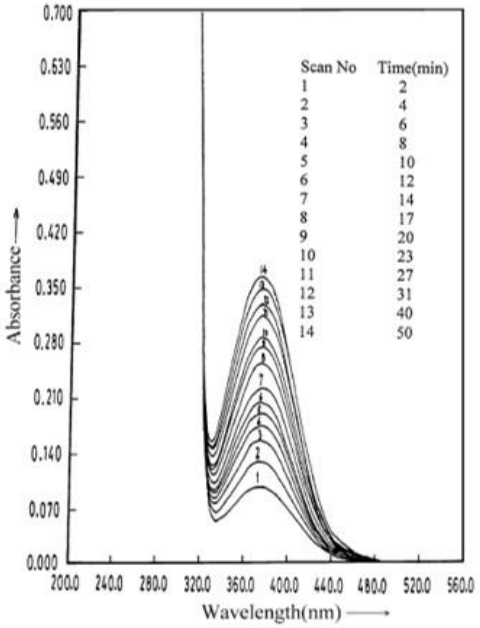

Figure 1. The repetitive spectrum of the typical catalytic kinetic run.

Experimental Conditions: Temperature = 45.0 ± 0.1 ºC, $[Hg^{2+}] = 1.5 \times 10^{-4}$ M, I = 0.10 M (KCl), [Pyrazine] = 7.5×10^{-4} M, pH = 4.0 ± 0.02, and $[Ru(CN)_6^{4-}] = 5.25 \times 10^{-5}$ M.

The spectral changes of the typical catalytic kinetic run recorded between 200-560 nm clearly depict that only one product $[Ru(CN)_5Pz]^{3-}$ is formed in the reaction. The continuous hike in absorbance observed at 370 nm is ascribed to the increase in the concentration of $[Ru(CN)_5Pz]^{3-}$ complex (Fig. 1).

The effect of distinct process parameters viz. ionic strength, temperature, [catalyst], pH, and [reactants] on the reaction rate was studied to optimize the reaction condition. Pseudo-first-order condition was maintained by taking minimum 10 fold excess of [pyrazine] over $[Ru(CN)_6^{4-}]$ throughout the kinetic investigation.

3.1. Optimization of reaction conditions.

3.1.1. Influence of pH on the initial reaction rate.

The previous reports on cyanide imitation with nitrogen heterocyclic ligands from $[Ru(CN)_6]^{4-}$ clearly indicate that pH is one of the key parameters which firmly influences the reaction rate [23,24.51]. To get the optimum pH condition, pH was varied from 2.0 to 6.5, and absorbance was recorded at a fixed time of 10 and 15 min after the sequential mixing of reagents (Fig. 2).

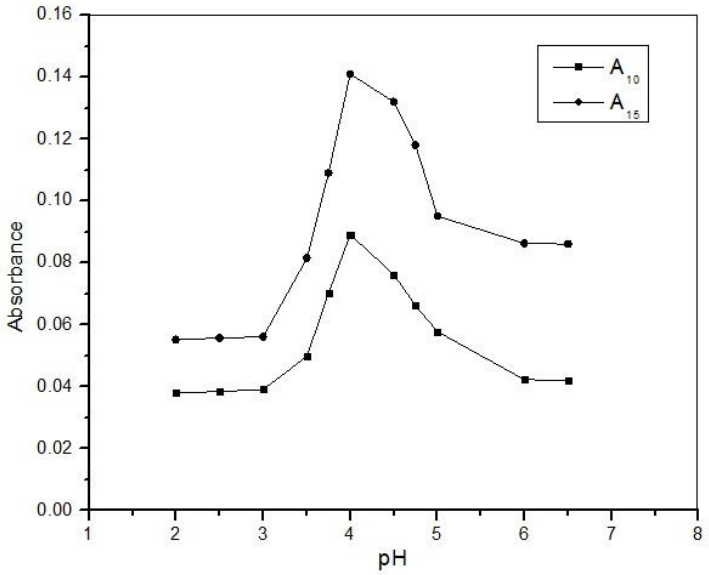

Figure 2. Influence of pH on the initial reaction rate.

Experimental Conditions: Temperature = 45.0 ± 0.1 ºC, $[Hg^{2+}] = 1.5 \times 10^{-4}$ M, I = 0.10 M (KCl), [Pyrazine] = 7.5×10^{-4} M, and $[Ru(CN)_6^{4-}] = 5.25 \times 10^{-5}$ M

The figure depicts that the substitution rate increases very sharply with pH from 3.25, attains its maximum value at ~ 4.0, decreases steeply from pH ~ 4.0 to 5.5, and then remains unaltered with a further increase in pH up to 6.5. The production of $[(HCN)Ru(CN)_4OH_2]^{2-}$, the less reactive protonated species of cyanide, is the possible reason for the sharp decline in the initial rate at lower pH. Furthermore, the predominant existence of a diprotonated form of pyrazine and tetra-protonated hexacyanoruthenate(II) ($H_4[Ru(CN)_6]$) in strong acidic condition will reduce the effective concentration of pyrazine and $[Ru(CN)_6]^{4-}$ thereby resulting in a reduced rate [51,52].

The predominant existence of a deprotonated form of pyrazine and hexacyanoruthenate(II) at higher pH reduces the availability of H^+ [51,52]. The decreased rate at higher pH can be ascribed to the scarcity of H^+ ions necessary for the regeneration of catalytic moiety and/or the possible hydrolytic precipitation of catalyst as hydroxide [23]. The lower regeneration of catalyst Hg^{2+} and its precipitation as hydroxide decreases the effective concentration of Hg(II) and, therefore, the reaction rate.

3.1.2. Influence of [pyrazine] on the initial reaction rate.

The optimized pH (4.0 ± 0.02) at 45 ºC temperature, under pseudo-uni-molecular reaction condition (by taking excess of pyrazine over $[Ru(CN)_6^{4-}]$), was applied to examine the impact of [pyrazine] on the substitution rate. The initial rate of reaction was evaluated in the varied concentration range of pyrazine (8.0×10^{-6} to 1.0×10^{-3} M) while fixing the other reaction parameters at a constant value. The graph of the initial rate against [pyrazine], presented in figure 3 states that the reaction rate increases with an increase in [pyrazine], reaches the maximum at 7.5×10^{-4} M, and further decreases in the studied concentration range of pyrazine. The lower rate at higher [pyrazine] is due to the lower availability of the catalyst as the Hg-pyrazine complex's formation decreases the effective concentration of Hg(II). The predominant existence of diprotonated species of pyrazine at its low concentration may be the possible reason for the slowness of reaction at lower [pyrazine] [52].

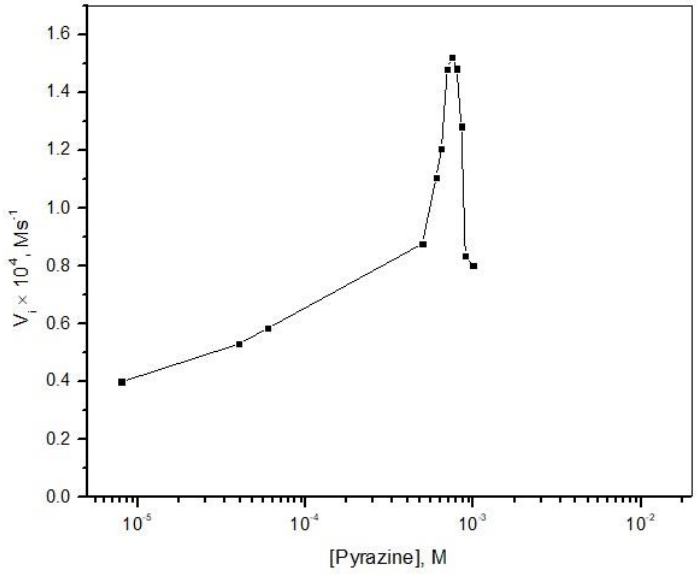

Figure 3. Influence of [Pyrazine] on the initial reaction rate.

Experimental Conditions: Temperature = 45.0 ± 0.1 ºC, $[Hg^{2+}] = 1.5 \times 10^{-4}$ M, I = 0.10 M (KCl), pH = 4.0 ± 0.02, and $[Ru(CN)_6^{4-}] = 5.25 \times 10^{-5}$ M

3.1.3. Influence of $[Ru(CN)_6^{4-}]$ on the initial reaction rate.

To examine the influence of $[Ru(CN)_6^{4-}]$ on cyanide substitution rate, we vary $[Ru(CN)_6]^{4-}$ concentration from 2.3×10^{-5} to 1.0×10^{-4}, confining the other process parameters at a constant value. The graph plotted between $\log V_i$ versus $\log[Ru(CN)_6^{4-}]$ speculates variable order kinetics in the studied concentration range of $[Ru(CN)_6]^{4-}$ (Fig. 4). The reaction exhibits first-order kinetics at a lower $[Ru(CN)_6^{4-}]$, becomes fractional-order when the $[Ru(CN)_6^{4-}]$ is more than 7.5×10^{-5} but not inclined towards zero-order kinetics.

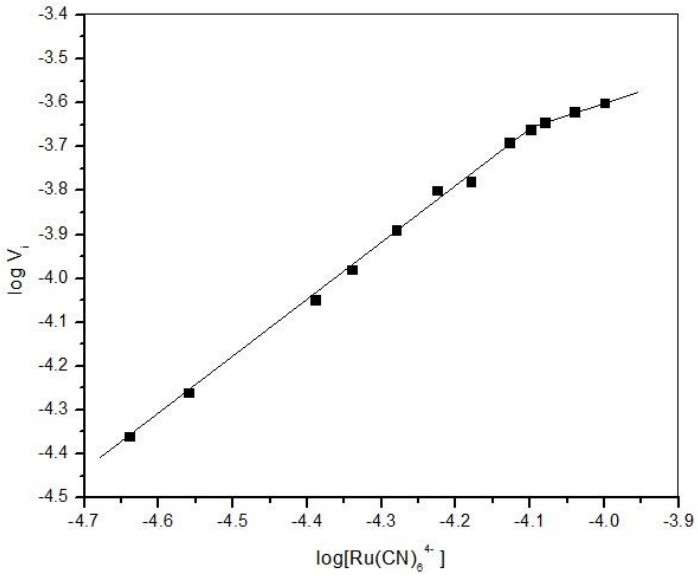

Figure 4. Influence of $[Fe(CN)_6^{4-}]$ on the initial reaction rate.

Experimental Conditions: Temperature = 45.0 ± 0.1 ºC, $[Hg^{2+}] = 1.5 \times 10^{-4}$ M, I = 0.10 M (KCl), [Pyrazine] = 7.5×10^{-4} M, and pH = 4.0 ± 0.02.

3.1.4. Influence of [electrolyte] and temperature on the initial reaction rate.

The impact of electrolyte concentration on the reaction rate was examined by varying the ionic strength (0.025 to 0.25) using potassium chloride at 45 °C keeping $[Hg^{+2}] = 1.5 \times 10^{-4}$ M, [pyrazine] = 7.5×10^{-4} M, pH = 4.0 ± 0.02, and $[Ru(CN)_6^{4-}] = 5.25 \times 10^{-5}$ M. The observed decreasing trend in the initial rate with increasing electrolyte concentration is due to the negative salt effect (Fig. 5).

The influence of temperature on the Hg^{2+} promoted cyanide exchange rate with pyrazine from $[Ru(CN)_6^{4-}]$ was inspected in the temperature range of 30-50 ºC. The reaction was not attempted at higher temperature due to the possible degradation of substitution product, $([Ru(CN)_5Pz]^{3-})$ formed during the reaction, also at a higher temperature, the reaction proceeds at a very fast rate, and thus no significant change was observed in $\ln(A_\infty - A_t)$ value. As expected reaction rate increases with the temperature rise. 45 ºC was considered as an optimum reaction temperature as the substitution reaction proceeds smoothly with a reasonable rate at that particular temperature.

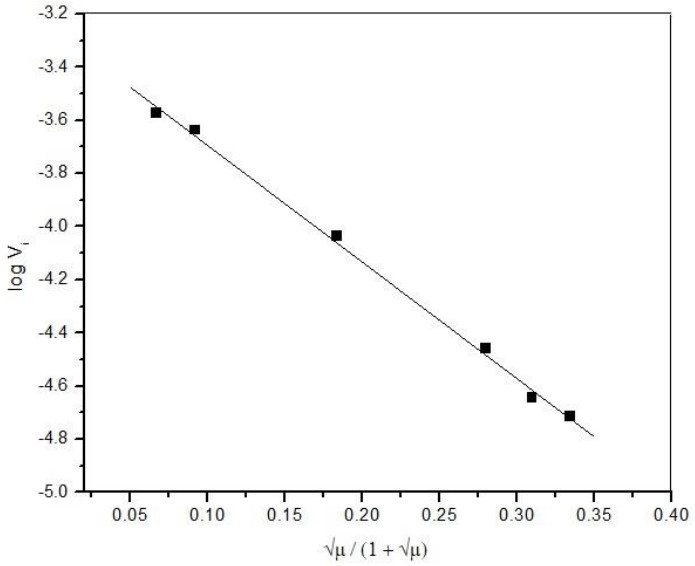

Figure 5. Influence of electrolyte concentration on the initial reaction rate.

Experimental Conditions: Temperature = 45.0 ± 0.1 ºC, $[Hg^{2+}] = 1.5 \times 10^{-4}$ M, [Pyrazine] = 7.5×10^{-4} M, pH = 4.0 ± 0.02, and $[Ru(CN)_6^{4-}] = 5.25 \times 10^{-5}$ M

3.1.5. Influence of $[Hg^{2+}]$ on the initial reaction rate.

The investigation of [catalyst] (Hg^{2+}) variation on the initial rate of the reaction is significant as the high catalytic efficiency of Hg^{2+} at its lower concentration can be immediately applied in the trace level estimation of Hg^{2+} in distinct water samples [50,53]. To study the varying role of Hg^{2+} on substitution rate, the absorbance after 10 min of mixing of the reactants under specified reaction condition (Temperature = 45.0 ± 0.1 ºC, I = 0.05 M {KCl}, [pyrazine] = 7.5×10^{-4} M, pH = 4.0 ± 0.02, and $[Ru(CN)_6^{4-}] = 5.25 \times 10^{-5}$ M) was recorded at different $[Hg^{2+}]$ ranging from 1.0×10^{-7} M to 6.0×10^{-4} M. The graph plotted between absorbance with $[Hg^{2+}]$ (Fig. 6) exhibits a linear dependency at lower $[Hg^{2+}]$. With further increase in $[Hg^{2+}]$, the initial reaction rate increases in a non-linear manner until $[Hg^{2+}]$ and $[Ru(CN)_6^{4-}]$ becomes approximately equal. The intercept obtained on the Y-axis through the extra-plotation of the

curve administers the uncatalyzed substitution reaction rate. At higher $[Ru(CN)_6^{4-}]$, white precipitate occurs immediately after the mixing of Hg^{2+} and $[Ru(CN)_6]^{4-}$ in a minimum 2:1 mole ratio. The growth in initial rate with $[Hg^{2+}]$ up to 1×10^{-4} M can be ascribed to the binuclear adduct formed between $[Ru(CN)_6]^{4-}$ and Hg^{2+} [50]. The absorption of cyanide by Hg^{2+} leads to the production of more labile $[Ru(CN)_5H_2O]^{3-}$, which then reacts very rapidly with pyrazine to form the final substitution product. The enhanced abstraction of CN^- by Hg^{2+} is responsible for the sharp decline in the initial reaction rate at higher $[Hg^{2+}]$ when the ratio of $[Hg^{2+}]/[Ru(CN)_6^{4-}] \geq 2$ the complete abstraction of CN^- by Hg^{2+} leads to the formation of Ru^{2+}.

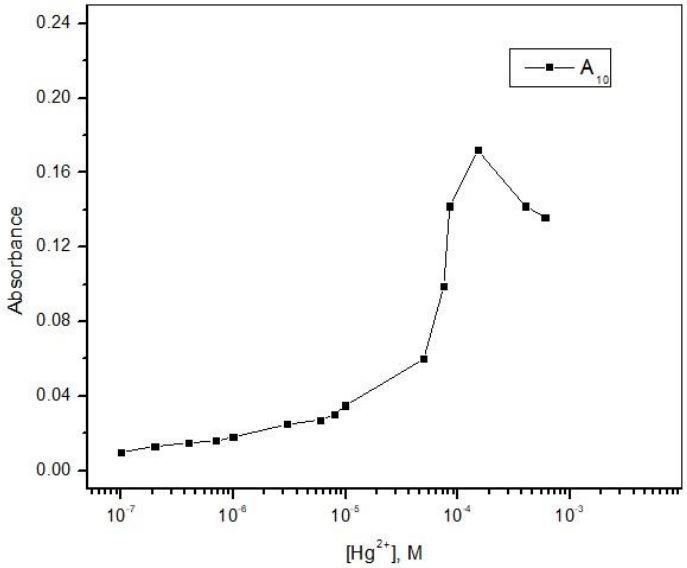

Figure 6. Influence of $[Hg^{2+}]$ on the initial reaction rate.

Experimental Conditions: Temperature = 45.0 ± 0.1 ºC, I = 0.05 M (KCl), [Pyrazine] = 7.5×10^{-4} M, pH = 4.0 ± 0.02, and $[Ru(CN)_6^{4-}] = 5.25 \times 10^{-5}$ M

3.2. Kinetic determination of D-penicillamine.

The previous reports on sodium thiosulphate, thioglycolic acid, and methionine reveal that the sulfur compounds inhibit the Hg^{2+} catalyzed substitution rate of cyanide from $[Ru(CN)_6]^{4-}$ by nitrogen donor incoming ligand [39-41]. The rate of investigated reaction will also decrease by adding D-penicillamine as it forms a stable catalyst–inhibitor [Hg^{2+}---- D-PCN] complex with Hg^{2+}. The formation of this complex reduces the effective concentration of Hg^{2+} that ultimately results in the loss of its catalytic activity. A proportional decrease in the reaction rate was observed with the inclusion of D-PCN. The change in absorbance (A_t) after 15 and 20 min of mixing of reactants with varying [D-PCN] (1.0×10^{-6} M to 10×10^{-5} M) was recorded under optimum reaction conditions. The graph plotted between A_t and [D-PCN] exhibits a linear relationship in the concentration range of 1.0×10^{-5} M to 10×10^{-5} M (Fig. 7). The plot can be used as a calibration curve for the quantitative estimation of D-PCN. The expressions relating A_t and [D-PCN] can be represented as Eq.1 and 2.

$$A_{15} = 0.128 - 1.143 \times 10^{3}[D - PCN] \quad (1)$$

$$A_{20} = 0.161 - 1.429 \times 10^{3}[D - PCN] \quad (2)$$

The graph plotted between A_t and [D-PCN] exhibits standard deviation and linear regression coefficient of 0.002, 0.0008, and 0.9981, 0.9963 for A_{15} and A_{20}. Recovery experiments for D-PCN determination were performed by taking a calculated amount of D-PCN in distilled water to check the current method's accuracy and reproducibility. Table 1 shows the recovered D-PCN along with standard deviation and percentage error. The D-PCN can be quantitatively determined up to 1.0×10^{-6} M level by the proposed analytical method.

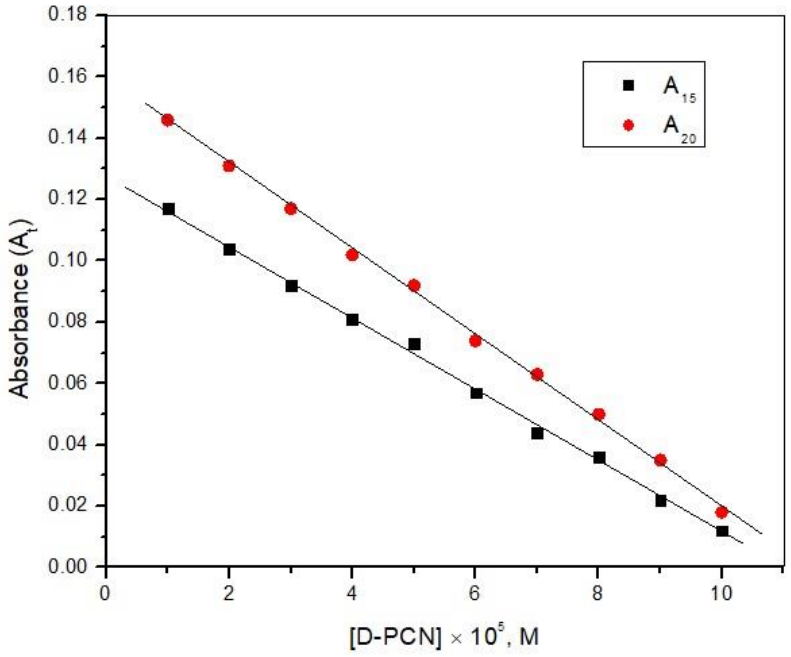

Figure 7. Calibration curve for the D-Penicillamine determination.

Experimental Conditions: Temperature = 45.0 ± 0.1 ºC, $[Hg^{2+}] = 1.5 \times 10^{-4}$ M, I = 0.10 M (KCl), [Pyrazine] = 7.5×10^{-4} M, pH = 4.0 ± 0.02, and $[Ru(CN)_6^{4-}] = 5.25 \times 10^{-5}$ M

Table 1. Recovery results and % error for D-PCN determination.
Experimental Conditions: Temperature = 45.0 ± 0.1 ºC, $[Hg^{2+}] = 1.5 \times 10^{-4}$ M, I = 0.10 M (KCl), [pyrazine] = 7.5×10^{-4} M, pH = 4.0 ± 0.02, and $[Ru(CN)_6^{4-}] = 5.25 \times 10^{-5}$ M

[D-PCN]×10^5 M (Taken)	**A_{15}**		**A_{20}**	
	[D-PCN]×10^5 M (Recovered)	**% Error**	**[D-PCN]×10^5 M (Recovered)**	**% Error**
1.03	1.05 ± 0.04	+ 0.019	1.00 ± 0.03	− 0.030
1.25	1.24 ± 0.08	− 0.008	1.28 ± 0.04	+ 0.023
1.76	1.76 ± 0.00	0.000	1.73 ± 0.06	− 0.017
2.10	2.09 ± 0.05	− 0.005	2.10 ± 0.00	0.000
2.52	2.50 ± 0.01	− 0.008	2.55 ± 0.08	+ 0.012
2.85	2.88 ± 0.07	+ 0.010	2.81 ± 0.07	− 0.014
4.50	4.58 ± 0.12	+ 0.021	4.51 ± 0.02	+ 0.011
7.50	7.41 ± 0.09	− 0.019	7.45 ± 0.07	− 0.016

To acknowledge the inhibition induced by sulfur donor ligand, D-PCN on Hg^{2+} catalyzed exchange of cyanide with pyrazine from $[Ru(CN)_6]^{4-}$, a modified mechanistic scheme has been proposed by equations (3) – (7) (Scheme 1). The current reaction system in hand produces more accurate results for the D-PCN determination as the uncatalyzed reaction between pyrazine and hexacyanoruthenate(II) is insignificant under the stipulated experimental condition (not presented in the proposed scheme) [51].

3.3. Interference of co-existing components.

The influence of excipients, which are usually present along with drugs in pharmaceutical preparations, was checked by performing the recovery experiments from the solution containing 4.0 μgml^{-1} D-PCN under the optimum reaction condition and a large number of diverse species. The recovery results using the A_{15} calibration curve suggest that the addition of excipients even up to 1000 times with the [D-PCN] does not significantly interfere with the determination of D-PCN (Table 2).

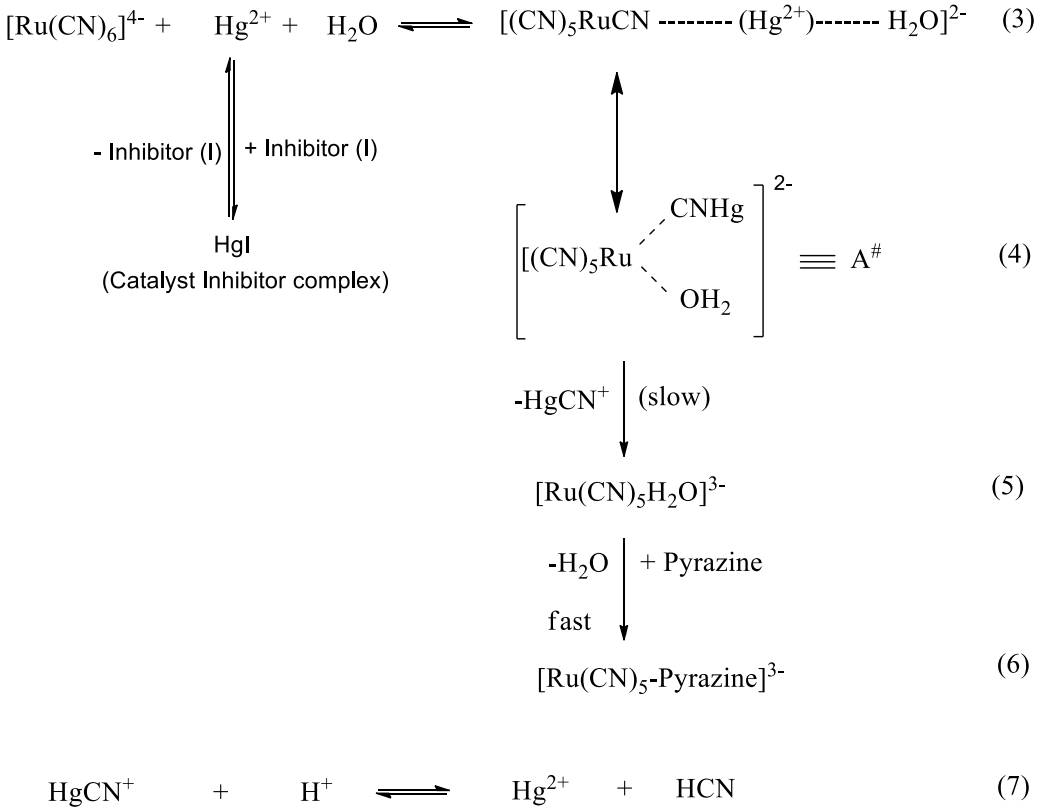

Scheme 1. Plausible mechanism

Table 2. Recovery results of D-Pencilliamine (4.0 μg ml^{-1}) in the presence if excipients.
Experimental Conditions: Temperature = 45.0 ± 0.1 ºC, [Hg^{2+}] = 1.5 × 10^{-4} M, I = 0.10 M (KCl), [pyrazine] = 7.5 × 10^{-4} M, pH = 4.0 ± 0.02, and [$Ru(CN)_6^{4-}$] = 5.25 × 10^{-5} M

Additives	[Additives] / [D-PCN]	Recovery ± RSD (%)
Sodium alginate	500	100.7 ± 0.5
Calcium sulphate	1000	99.5 ± 0.8
Starch	500	100.6 ± 0.7
Magnesium stearate	500	99.6 ± 0.3
Lactose	500	100.6 ± 0.5
Citrate	1000	99.8 ± 0.2
Glactose	1000	100.2 ± 0.6
Glucose	1000	99.7 ± 0.4

3.4. Application in pharmaceutical preparations.

The proposed kinetic spectrophotometric method was effectually employed for the quantitative determination of D-PCN in pharmaceutical samples. D-PCN's content from 10 capsule/tablet was finally grounded and dissolved in 100 ml of deionized distilled water, which after sonication for 20 min was filtered off using Whatman filter paper. The solution was further

diluted with deionized distilled water to bring [D-PCN] within the calibration range. Five different pharmaceutical samples of D-PCN (capsule/tablet) were subjected to the spectrophotometric determination of D-PCN. The statistical comparison of the result obtained by the designed method with the standard method indicates the developed method's precision and accuracy for D-PCN determination (Table 3) [54].

The mean recovery (99-101) demonstrates that the proposed analytical method can be effectively employed for the quick quantitative estimation of D-PCN in the pharmaceutical samples with good accuracy and reproducibility.

Table 3. Determination of D-PCN in Pharmaceutical samples and statistical comparison with the official method.

Experimental Conditions: Temperature = 45.0 ± 0.1 ºC, $[Hg^{2+}] = 1.5 \times 10^{-4}$ M, I = 0.10 M (KCl), [pyrazine] = 7.5×10^{-4} M, pH = 4.0 ± 0.02, and $[Ru(CN)_6^{4-}] = 5.25 \times 10^{-5}$ M

Pharmaceutical Samples	Proposed Method Recovery ± RSD (%)	Official Method Recovery ± RSD (%)
Aaramine 250 mg Capsule (RR life science Pvt. Ltd.)	100.46 ± 0.69	99.94 ± 0.38
Pendramine 250 mg Tab. (Kent Pharmaceuticals Ltd.)	101.02 ± 0.52	99.94 ± 0.38
Artin 150 mg Capsules (Arvinol Laboratories Pvt. Ltd.)	99.53 ± 0.73	99.94 ± 0.38
D Penamine 125 mg Tab. (Alphapharm)	100.68 ± 0.39	99.94 ± 0.38
D-Penicillamine 150 mg Capsule (Taj Pharma)	99.62 ± 0.48	99.94 ± 0.38

4. Conclusions

Using the inhibitory effect of sulfur compounds towards Hg(II), a new, rapid, and accurate kinetic spectrophotometric method was developed to determine D-PCN quantitatively. The current reaction system in hand produces more accurate results for the D-PCN determination. The uncatalyzed reaction between pyrazine and hexacyanoruthenate(II) is insignificant under the stipulated experimental condition. The inclusion of D-PCN only reduces the rate of substitution reaction. The addition of common excipients in pharmaceuticals even up to 1000 times with the [D-PCN] has no significant interference in the determination of D-PCN. The D-PCN can be quantitatively determined up to 1.0×10^{-6} M level by the proposed analytical method. The statistical comparison of the result obtained by the designed method with the standard method indicates that the proposed methodology can be convincingly adopted for the rapid determination of D-PCN in the pharmaceutical preparations with good accuracy and reproducibility.

Funding

This research received no external funding.

Acknowledgments

This research has no acknowledgment.

Conflicts of Interest

The authors declare no conflict of interest.

References

1. Tang, K. Chemical Diversity and Biochemical Transformation of Biogenic Organic Sulfur in the Ocean. **2020**, *7*, https://doi.org/10.3389/fmars.2020.00068.
2. Abadie, C.; Tcherkez, G. Plant sulphur metabolism is stimulated by photorespiration. *Communications Biology* **2019**, *2*, https://doi.org/10.1038/s42003-019-0616-y.
3. Kolluru, G.K.; Shen, X.; Kevil, C.G. Reactive sulfur species: a new redox player in cardiovascular pathophysiology. *Arterioscler Thromb Vasc Biol* **2020**, *40*, 874-884, https://doi.org/10.1161/ATVBAHA.120.314084.
4. Fukuto, J.M.; Ignarro, L.J.; Nagy, P.; Wink, D.A.; Kevil, C.G.; Feelisch, M.; Cortese-Krott, M.M.; Bianco, C.L.; Kumagai, Y.; Hobbs, A.J. *et al*.. Biological hydropersulfides and related polysulfides-a new concept and perspective in redox biology. *FEBS Lett* **2018**, *592*, 2140–2152, https://doi.org/10.1002/1873-3468.13090.
5. Eidelman, C.; Lowry, J.A. D-Penicillamine. In: *Critical Care Toxicology. Springer Cham*. Brent, J.; Burkhart, K.; Dargan, P.; Hatten, B.; Megarbane, B.; Palmer, R. (eds), **2016**; pp. 1-7.
6. Litwin, T.; Czlonkowska, A.; Socha, P. Oral chelator treatment of wilson disease: d-penicillamine. *Clinical and Translational Perspectives on WILSON disease* **2019**, 357-364, https://doi.org/10.1016/B978-0-12-810532-0.00034-3.
7. Chang, H.; Xu, A.; Chen, Z.; Zhang, Y.; Tian, F.; Li, T. Long-term effects of a combination of D-penicillamine and zinc salts in the treatment of Wilson's disease in children. *Exp Ther Med* **2013**, *5*, 1129-1132, https://doi.org/10.3892/etm.2013.971.
8. Kianoush, S.; Mood, M.B.; Mousavi, S.R. Comparison of therapeutic effects of garlic and d-penicillamine in patients with chronic occupational lead poisoning. *Basic Clin Pharmacol* **2011**, *110*, 476-81, https://doi.org/10.1111/j.1742-7843.2011.00841.x.
9. Sisombath, N.S.; Lalilehvand, F.; Schell, A.C.; Wu, Q. Lead(II) binding to the chelating agent d-penicillamine in aqueous solution. *Inorg. Chem* **2014**, *53*, 12459–12468, https://doi.org/10.1021/ic5018714.
10. Shannon, M.V.; Townsens, M.W. Adverse effects of reduced-dose d-penicillamine in children with mild-to-moderate lead poisoning. *Ann Pharmacother* **2000**, *34*, 15-8, https://doi.org/10.1345/aph.19084.
11. Liu, X.; Ding, W.; Wu, Y.; Zeng, C.; Luo, Z.; Fu, H. Penicillamine-protected Ag_{20} nanoclusters and fluorescence chemosensing for trace detection of copper ions. *Nanoscale* **2017**, *9*, 3986-3994, https://doi.org/10.1039/C6NR09818E.
12. Hong, Y.; Jo, S.; Park, J.; Park, J.; Yang, J. High sensitive detection of copper II ions using D-penicillamine-coated gold nanorods based on localized surface plasmon resonance. *Nanotechnology* **2018**, *29*, https://doi.org/10.1088/1361-6528/aab4c4
13. Panahi, P.P.; Hasanzadeh, M.; Keihan, R.E. A novel optical probe based on d-penicillamine-functionalized graphene quantum dots: Preparation and application as signal amplification element to minoring of ions in human biofluid. *J Mol Recognit* **2020**, *33*, https://doi.org/10.1002/jmr.2828.
14. Jullien, A.S.; Gateau, C.; Lebrun, C.; Kieffer, I.; Testemale, D.; Delangle, P. D-penicillamine tripodal derivatives as efficient copper(I) chelators, *Inorg Chem* **2014**, *53*, 5229-5239, https://doi.org/10.1021/ic5004319.
15. Zhang, X.; Liu, Q.; Wang, Z.W.; Xu, H.; An, F.P.; Huang, Q.; Song, H.B.; Wang, Y.W. D-penicillamine modified copper nanoparticles for fluorometric determination of histamine based on aggregation-induced emission. *Microchimica Acta* **2020**, *187*, https://doi.org/10.1007/s00604-020-04271-1
16. Layton, M.A.; Jones, P.W.; Alldersea, J.E.; Strange, R.C.; Fryer, A.A.; Dawes, P.T.; Mattey, D.L. The therapeutic response to D-penicillamine in rheumatoid arthritis: influence of glutathione S-transferase polymorphisms. *Rheumatology* **1999,** *38*, 43-47, https://doi.org/10.1093/rheumatology/38.1.43.
17. Omondi, R.O.; Stephen, O.; Ojwach, S.O.; Jaganyi, D. Review of comparative studies of cytotoxic activities of Pt(II), Pd(II), Ru(II)/(III) and Au(III) complexes, their kinetics of ligand substitution reactions and DNA/BSA interactions. *Inorg Chim Acta* **2020**, *512*, https://doi.org/10.1016/j.ica.2020.119883.
18. Naik, R.M.; Srivastava, A.; Asthana, A. The kinetics and mechanism of oxidation of hexacyanoferrate(II) by periodate ion in highly alkaline aqueous medium. *J Iran Chem Soc* **2008**, *5*, 29-36, https://doi.org/10.1007/BF03245812.
19. Iioka, T.; Takahashi. S.; Yoshida, Y.; Matsumura, Y.; Hiraoka, S.; Sato, H. A kinetics study of ligand substitution reaction on dinuclear platinum complexes: Stochastic versus deterministic approach. *J Comput Chem* **2019**, *40*, 279-285, https://doi.org/10.1002/jcc.25588.
20. Naik, R.M.; Srivastava, A.; Verma, A.K.; Yadav, S.B.S.; Singh, R.; Prasad, S. The kinetics and mechanism of oxidation of triethylenetetraaminehexaacetate. *Bioinorg Reac Mech* **2007**, *6*, 185-192, https://doi.org/10.1515/IRM.2007.6.3.185.
21. Srivastava, A.; Sharma, V.; Prajapati, A.; Srivastava, N.; Naik, R.M. Spectrophotometric determination of ruthenium utilizing its catalytic activity on oxidation of hexacyano ferrate(II) by periodate ion in water samples. *Chem Chem Technol* **2019**, *13*, 275-279, https://doi.org/10.23939/chcht13.03.275.

22. Prasad, S.; Naik, R.M.; Srivastava, A. Application of ruthenium (III) catalyzed oxidation of Tris(2-amino ethyl) amine in trace determination of ruthenium in environmental water samples. *Spectrochim Acta A* **2008,** *70*, 958-65, https://doi.org/10.1016/j.saa.2007.10.011.
23. Rastogi, R.; Srivastava, A.; Naik, R.M. Kinetic and mechanistic analysis of ligand substitution of aquapentacyanoruthenate(II) in micelle medium by nitrogen donor heterocyclic ligand. *J Disp Sc Tech* **2020**, *41*, 1045-1050, https://doi.org/10.1080/01932691.2019.1614042.
24. Srivastava, A.; Naik, R.M.; Rastogi, R. Spectrophotometric kinetic study of mercury(II) catalyzed formation of $[4\text{-CN-PyRu(CN)}_5]^{3-}$ via ligand exchange reaction of hexacyanoruthenate(II) with 4-cyanopyridine – a mechanistic approach. *J Iran Chem Soc* **2020,** *17*, 2327-2333, https://doi.org/10.1007/s13738-020-01927-w
25. Huang, Y.; Lin, T.; Hou, L.; Ye, F.; Zhao, S. Colorimetric detection of thioglycolic acid based on the enhanced Fe^{3+} ions Fenton reaction. *Microchem J* **2019**, *144*, 190–194, https://doi.org/10.1016/j.microc.2018.09.003.
26. Dedov, A.G.; Marchenko, D.Y.; Zrelova, L.V.; Ivanova, E.A.; Sandzhieva, D.A.; Parkhomenko, A.A.; Budinov, S.V.; Lobakova, E.S.; Dol'nikova, G.A. New Method for Determination of Total of Organic Sulfur Compounds in Hydrocarbon Media. *Petroleum Chemistry* **2018**, *58*, 714-720, https://doi.org/10.1134/S0965544118080030.
27. Kostara, A.; Tsogas, G.Z.; Vlessidis, A.G.; Giokas, D.L. Generic Assay of Sulfur-Containing Compounds Based on Kinetics Inhibition of Gold Nanoparticle Photochemical Growth. *ACS Omega* **2018**, *3*, 16831-16838, https://doi.org/10.1021/acsomega.8b02804.
28. Raab, A.; Feldmann, J. Biological sulphur-containing compounds – Analytical challenges. *Anal Chim Acta* **2019**, *1079*, 20-29, https://doi.org/10.1016/j.aca.2019.05.064.
29. Zhand, S.; Jiang, J.Q. Detection of imidacloprid and Bisphenol-S by Solid Phase Extraction (SPE) coupled with UV-VIS spectrometer and LC-MS. *Biointerface Res Appl Chem* **2019**, 9, 4433-4438, https://doi.org/10.33263/BRIAC95.433438.
30. Ni, L.; Geng, X.; Li, S.; Ning, H.; Guan, Y. A flame photometric detector with a silicon photodiode assembly for sulfur detection. *Talanta* **2020**, *207*, https://doi.org/10.1016/j.talanta.2019.120283.
31. Nelson, J. Nuclear magnetic resonance spectroscopic method for determination of penicillamine in capsules. *J Assoc Off Anal Chem* **1981**, *64*, 1174-1178, https://doi.org/10.1093/jaoac/64.5.1174.
32. Chao, Q.; Sheng, H.; Cheng, X.; Ren, T. Determination of sulfur compounds in hydrotreated transformer base oil by potentiometric titration. *Ana Sci* **2005**, *21*, 721-724, https://doi.org/10.2116/ANALSCI.21.721.
33. Shoba, S.; Bankole, O.M.; Ogunlaja, A.S. Electrochemical determination of trace sulfur containing compounds in model fuel based on a silver/polyaniline-modified electrode. *Anal Methods* **2020**, *12*, 1094-1106, https://doi.org/10.1039/C9AY02382H.
34. Nugrahani, I.; Abotbina, I.M.; Apsari, C.N.; Kartavinata, T.G.; Sukranso.; Oktaviary, R. Spectrofluorometric determination of L-tryptophan in canary (Canarium indicum L.) seed protein hydrolysate. *Biointerface Res Appl Chem* **2019**, *10*, 4780-4785, https://doi.org/10.33263/BRIAC101.780785.
35. Perez-Ruiz, T.; Martinez- Lozano, C.; Tomas, V.; Sidrach-de-Fardona, C. Flow-injection fluorimetric determination of penicillamine and tiopronin in pharmaceutical preparations. *J Pharm Biomed Anal* **1996**, *15*, 33-38, https://doi.org/10.1016/0731-7085(96)01821-3
36. Feng, G.; Sun, S.; Wang, M.; Zhao, Q.; Liu, L.; Hashi, Y.; Jia, R. Determination of four volatile organic sulfur compounds by automated headspace technique coupled with gas chromatography–mass spectrometry. *J Water Supply Res T* **2018**, *67*, 498–505, https://doi.org/10.2166/aqua.2018.011.
37. Dzieko, U.; Kubczak, N.; Przybylska, K.P.; Patalski, P.; Balcerek, M. Development of the method for determination of volatile sulfur compounds (vscs) in fruit brandy with the use of HS–SPME/GC–MS. *Molecules* **2020**, *25*, https://doi.org/10.3390/molecules25051232.
38. Cao, L.; Wei, T.; Shi, Y.; Tan, X.; Meng, J. Determination of D-penicillamine and tiopronin in human urine and serum by HPLC-FLD and CE-LIF with 1,3,5,7-tetramethyl-8-bromomethyl-difluoroboradiaza-s-indacene. *J Liq Chrom Relat Tech* **2018**, *41*, 58-65.
39. Srivastava, A. Micro-level estimation of Mercaptoacetic acid using its inhibitory effect to mercury catalyzed ligand exchange reaction of hexacyanoruthenate(II). *Biointerface Res Appl Chem* **2020,** *10*, 7152-7161, https://doi.org/10.33263/BRIAC106.71527161.
40. Agarwal, A.; Prasad, S.; Naik, R.M. Inhibitory kinetic spectrophotometric method for the quantitative estimation of D-penicillamine at micro levels. *Microchem J* **2016**, *128*, 181-186, https://doi.org/10.1016/j.microc.2016.04.005.
41. Srivastava, A. Micro-level Estimation of Methionine Using Inhibitory Kinetic Spectrophotometric Method. *Biointerface Res Appl Chem* **2021,** *11*, 10654-10663.
42. Yu, B.; Rees, T.W.; Liang, J.; Jin, C.; Chen, Y.; Ji, L.; Chao, H. DNA interaction of ruthenium(II) complexes with imidazo [4,5-*f*] [1,10] phenanthroline derivatives. *Dalton Trans* **2019**, *48*, 3914-21, https://doi.org/10.1039/C9DT00454H.
43. Lin, K.; Zhao, Z.Z.; Bo, H.B.; Hao, X.J.; Wang, J.Q. Applications of ruthenium complex in tumor diagnosis and therapy. *Pharmacol* **2018**, *9*, https://doi.org/10.3389/fphar.2018.01323.
44. Kenny, R.G.; Marmion, C.J. Toward multi-targeted platinum and ruthenium drugs—A new paradigm in cancer drug treatment regimens? *Chem Rev* **2019**, *119*, 1058-1137.

45. Bastos, C.M.; Gordon, K.A.; Ocain, T.D. Synthesis and immunosuppressive activity of ruthenium complexes. *Bioorg Med Chem Lett* **1998**, *8*, 147-150, https://doi.org/10.1016/s0960-894x(97)10205-0.
46. Gua, L.; Lia, X.; Ran, Q.; Kang, C.; Lee, C.; Shen, J. Antimetastatic activity of novel ruthenium (III) pyridine complexes. *Cancer Med* **2016**, *5*, 2850-2860, https://doi.org/10.2147/IJN.S131304.
47. Coverdale, J.P.C.; Carron, T.L.M.; Canelon, I.R. Designing ruthenium anticancer drugs: what have we learnt from the key drug candidates? *Inorganics* **2019**, *7*, https://doi.org/10.3390/inorganics7030031.
48. Athar, F.; Husain, K.; Abid, M.; Azam, A. Synthesis and anti-amoebic activity of gold(I), ruthenium(II), and copper(II) complexes of metronidazole. *Chem Biodiversity* **2005**, *2*, 1320-1330, htpps://dio.org/10.1002/cbdv.200590104.
49. Gomes-Junior, F.A.; Silva, R.S.; Lima, R.G.; Vannier-Santos, M.A. Antifungal mechanism of [RuIII(NH3)4catechol]$^{+}$ complex on fluconazole-resistant Candida tropicalis. *FEMS Microbio Lett* **2017**, *364*, https://doi.org/10.1093/femsle/fnx073.
50. Naik, R.M.; Singh, P.K.; Rastogi, R.; Singh, R.; Agarwal, A. Kinetic-catalytic and spectrophotometric determination of Hg(II) using its catalytic effect on ligand substitution reaction between hexacyanoferrate(II) and pyrazine. *Annali di Chimica* **2007**, *97*, 1169-1179, https://doi.org/10.1002/adic.200790103.
51. Naik, R.M.; Verma, A.K.; Agarwal, A.; Asthana, A. Kinetic and mechanistic study of the mercury(II)-catalyzed substitution of cyanide in hexacyanoruthenate(II) by pyrazine. *Trans. Met. Chem* **2009**, *34*, 209-215, https://doi.org/10.1007/s11243-008-9180-x.
52. Kamei, H. The proton magnetic resonance study of the protonation of pyrazine. *J. Phys. Chem* **1965**, *69*, 2791-2793, https://doi.org/10.1021/j100892a507.
53. Agarwal, A.; Verma, A.K.; Yoshida, M.; Naik, R.M.; Prasad, S. A novel catalytic kinetic method for the determination of mercury(II) in water samples. *RSC Adv* **2020**, *10*, 25100-25106, https://doi.org/10.1039/d0ra03487h.
54. US Pharmacopeia, XXII Revision, *US Pharmacopeia Convention*. Rockville, MD, **1989**; pp. 1022-1024.